A novel statistical signal processing method to estimate effects of compounds on contractility of cardiomyocytes using impedance assays

Lévy Batista, Thierry Bastogne, Annie Delaunois, Jean-Pierre Valentin, Franck Atienzar

A novel statistical signal processing method to estimate effects of compounds on contractility of cardiomyocytes using impedance assays

L. Batista[a,b,d], T. Bastogne[a,b,c,d], A. Delaunois[e], J.-P. Valentin[e], F. Atienzar[e]

[a] *Université de Lorraine, CRAN, UMR 7039, Vandœuvre-lès-Nancy, France*
[b] *CNRS, CRAN, UMR 7039, Vandœuvre-lès-Nancy, France*
[c] *INRIA, BIGS, France*
[d] *CYBERnano, 193 avenue Paul Muller, 54602 Villers-lès-Nancy, France*
[e] *UCB Biopharma SPRL, Chemin du Foriest, B-1420 Braine-l'Alleud, Belgium*

Abstract

Label free methods such as cell impedance assays are *in vitro* tests increasingly used in drug development and producing large and high-content data files. Since the current commercial software are not suited for fully automated analysis, there is a need to develop validated and rapid solutions to extract relevant information for biologists. This need is particularly obvious in the case of impedance signals analysis from cardiomyocytes. The proposed solution is based on three main steps. The first one consists in calculating five indices informing about the time variations of frequency (F), amplitude (A), shape (S) of beatings, trends (T) of the cardiomyocyte dependent on spreading, viability and attachment as well as irregularity (I) of the contractility. In a second phase, two summary statistics are proposed to test the concentration effect of drugs on the five FASTI indices. Results of the statistical tests are finally aggregated in a cardio-effect grade to compare the tested molecules in a cardio-impact scale graduated from 0 (no influence) to 10 (highly disturbed effects in cardiomyocytes). This innovative approach was tested using *in vitro* data obtained from cell impedance analysis of three known molecules (2 cardiotoxic and 1 non-cardiotoxic compounds). Results have clearly shown the ability of the proposed approach to identify significant effects on the contractility of cardiomyocytes. This solution speeds up the analysis of cardiomyocyte impedance data, takes into account all the kinetic data generated and is now available for biologists on a web-platform: i-Cardio™ developed by CYBERnano™.

Keywords: signal processing, biostatistics, high-content screening, impedance, label-free technology, cardiomyocyte, cardiotoxicity.

1. Introduction

The CiPA[1] initiative [1, 2] aims at developing a new approach to assess the proarrhythmic potential of new chemical entities. So far, cardiovascular safety assessment was mainly focused on QT interval prolongation, which is used as a marker for predicting the risk of a compound to cause potentially fatal ventricular cardiac arrhythmia called Torsade de Pointes (TdP). The current preclinical safety guideline (ICH[2] S7B) relies on preclinical electrophysiology tests against hERG (*human-ether-à-go-go Related Gene*) and an *in vivo* QT measurement. Nevertheless, this approach may increase the number of false positive drugs. In addition, to increase the likelihood of success, an effective derisking strategy should evaluate proarrhythmia liability, hemodynamic cardiac contractility assessment, taking into account both functional and structural aspects of cardiotoxicity. All this situation has motivated ICH to reconsider approaches to the evaluation of drug-induced cardiac injuries. To that aim, *in silico* action potential simulations based on the O'Hara-Rudy model [3] have been integrated in the CiPA (Comprehensive In Vitro Proarrhythmia Assay) effort to better assess human cardiotoxicity risks. A second main component of the CiPA project relies on stem cell-derived human myocyte studies. Two technologies were suggested for evaluation, namely the multielectrode array (MEA) and the voltage-sensing optical (VSO) platforms. However, other emerging techniques exist, such as the cardiomyocyte impedance analysis, which proved to be useful to identify cardiotoxic compounds [4].

In this context, in the present paper, we evaluated the real-time cell analysis (RTCA) platform, measuring cell impedance, to assess effects on contractility of cardiomyocytes exposed to a small panel of drugs. By analogy, this approach may be compared with the detection and characterization of abnormalities in ECG signals. Mahmoud *et al.* [5] reported that the time-frequency distribution is employed to reveal the exact multicomponent structure of surface electromyogram with the presence of ECG noise and abnormal cardiac signals. Martis *et al.* (2014) compared four methods to diagnose ECG abnormalities [6]. They associate two different transforms (wavelet *vs* cosinus) with statistical techniques of reduction such as the Principal Component Analysis followed by clustering analysis involving K-nearest neighbor, decision tree and artificial neural networks. Since that time, a large spectrum of methods have been tested such as sequential Bayesian methods [7], multiscale energy and eigenspace approach [8], multiresolution time-dependent entropy method [9], signal decomposition model-based Bayesian approach [10] and continuous wavelet transform [11]. However, several main differences may be emphasized between the ECG and cardiomyocyte impedance analysis. Firstly, PQRST waves do not exist in CI (cell index) signals and their beating shape may change completely depending on the drugs used [12, 13]. Secondly, conversely to usual ECG that are recorded during about

[1] Comprehensive In Vitro Proarrhythmia Assay
[2] International Conference on Harmonisation

10s only, CI responses can be measured during one week of experimentation and generate larger data files to be processed.

MEA, VSO and RTCA platforms are increasingly used for drug discovery applications. In such a context, large number of molecules can be tested on cardiomyocytes and several parameters can be analyzed to assess cardiotoxicity risks. This computational task is time-consuming and user dependent. Our objective was to develop an automatic, reliable and fast method to compare the effects of tested drugs on cell impedance (CI) responses in cardiomyocytes. To address this issue, we propose a triple-stage method. The first step is based on the estimation of five time-variant parameters of CI responses. In a second phase, a concentration-effect modeling of the five indices is performed and statistical tests are used to assess the relevance of all variations in comparison with the control group. Finally, a score of critical effects is proposed to compare the alteration effects on the CI responses of tested molecules in a new cardio-impact scale. The second main intended purpose of this article is to assess the practical relevance of this new approach applied to real cardiomyocyte impedance data.

This paper is organized as follows. In section 2, the cardiomyocyte impedance analysis is introduced. Section 3 describes the methodology and the impedance data corresponding to three molecules are presented in section 4. Finally, as a proof of concept, results are discussed with a set of two cardiotoxic and one non-cardiotoxic compounds to demonstrate the potential of the developed approach to analyze impedance data in a rapid and reliable way.

2. Cardiomyocyte Impedance assays and summary of Material & Methods

The use of electrical impedance to measure cellular processes was first reported by Giaever in 1984, [14, 15]. The xCELLigence platform generating impedance data has been identified as a powerful and reliable tool in drug discovery for toxicity and pharmacology studies [16, 17]. All the impedance-based cell analyzers use the fact that cells have an electrical insulating membrane. This property comes from its biological composition. Indeed, the cell membranes are made of phospholipid bilayer, and these lipids act as electrical insulators, [18, 19]. Consequently, when an electrical current generated by electrodes at the bottom of a well flows into a ion solution, the whole well behaves as a variable impedance. The most cells fix on the substrat at the bottom of the wells, the most it decreases the current exchange area, increasing the impedance [18, 20]. This electrical impedance area is modified by multiple parameters including the number of cells, their size, the way cells communicate and spread, as well as their substrate adhesion. The data acquisition system (RTCA cardio) allows to get one numerical value of the cell impedance every $13ms$. The impedance value is finally transformed into dimensionless quantity entitled *Cell-index* (CI) [21, 22, 23]. These CI data generated by this technology provide two types of information: the viability of cardiomyocytes by examining the pattern of the impedance signal trend and the cardiomyocytes contractility by analyzing the periodic pattern of the impedance signals over short periods

called *sweeps*. As illustrated in Figure 1, the cell impedance sensing is sensitive enough to monitor cell spreading and clustering as well as beating of the cardiomyocytes. The spreading of the cells correspond to the increase in CI while the beating corresponds to the contraction of the cardiomyocytes. Those two phenomenons differ by amplitude and time constant. Indeed, the spreading is a slow and high amplitude process while the cardiac activity is a fast and slow amplitude process.

The measurement profile is recorded by a station on each well of a 96 wells plate. The data acquisition was split up into sweeps of 20 secondes recorded every 5 minutes. In each sweep, the sampling rate is equal to 77.35 Hz, resulting in a $K = 1547$ data-points by sweep. In other terms for control cardiomyocytes, each sweep contains around 28 beats and for a five-day measurement campaign, there are about 1440 sweeps to be processed for just one tested well. All the variables and parameters are listed in Table 1.

Symb.	Legend
$t \in [0, ..., T-1]$	moment of measurement of the $(t+1)$-th sweep
$k \in [0, ..., K-1]$	moment of CI measurement within each sweep
$y_t(k)$	$(k+1)$-th CI value in the t-th sweep
T	number of recorded sweeps
K	number of time points in a sweep signal
P	number of time points in a beating period
t_m	time of drug administration
$d \in [1, ..., D]$	index of the drug concentration
D	number of concentration (dose) levels
$r \in [1, ..., R]$	index of the replicated well
R	number of assay replications
Δt	time range of analysis after compound addition
$i \in [F, A, S, T, I]$	FASTI index
$F(t)$	beating mean frequency characteristic of the t-th sweep
$A(t)$	beating mean amplitude characteristic of the t-th sweep
$S(t)$	beating pattern characteristic of the t-th sweep
$T(t)$	t^{th} value of the CI trend, mean value of the t-th sweep
$I(t)$	beating irregularity feature of the t-th sweep

Table 1: Description of the parameters and variables used in the proposed statistical signal processing method

Mouse cardiomyocytes (inducible pluripotent stem cells) were purchased from Axiogenesis (Cologne, Germany). Famotidine (non-cardiotoxic drug) and Doxorubicine (cardiotoxic drug in humans) were ordered from Sigma-Aldrich (Saint-Louis, MO, USA), and Sunitinib (cardiotoxic drug in human) from VWR (Radnor, PA, USA). The mouse cardiomyocytes were thawed based upon Axiogenesis standard protocol and seeded on RTCA cardio E-plates at a density of $40 \cdot 10^3$ cells/well. To quantify cell status based on the measured cell-electrode impedance, a parameter termed cell index (CI) is derived. This index is a time

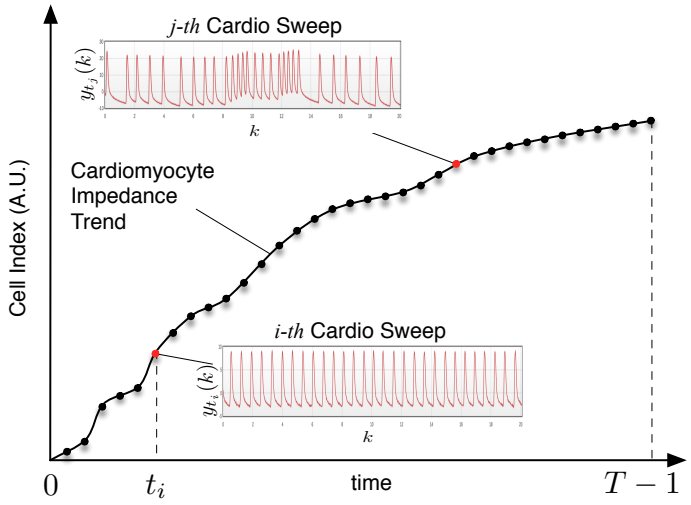

Figure 1: Real-time measurement of cardiomyocyte impedance responses. The trend response is measured the cell index (arbitrary unit) with a sampling period of about $5mn$. This increasing trend signal provides information about the cardiomyocyte attachment and spreading during the experimentation period. Zooming into the cell index response allows to monitor the contraction of the cardiomyocytes. At each time point t_i, a cardio-sweep is measured during $20s$ with a sampling rate of $77.35Hz$ to observe the cardiomyocyte beating pattern. k is the time index used in each cardio-sweep.

and sampling frequency dependent quantity described as follows:

$$CI(t_k, f_i) = \max_{i=1,2...k} \left[\frac{R_{cell}(t_k, f_i)}{R_{bg}(f_i)} - 1 \right] \quad (1)$$

where R_{bg} and R_{cell} are the resistances measured at time t_k and frequency f_i without and in presence of cells respectively [21, 22, 23]. N is the number of the frequency points at which the impedance is measured. For more details please refer to Atienzar et al. (2013) [17]. Cell index were monitored for a few days (usually 2 to 3 days) until all parameters measured were sufficiently stable (cell index, beating, amplitude, frequency, etc.). E-plates (Roche Diagnostics, Vilvoorde, Belgium) were coated, according to the manufacturer's recommendations. Fibronectin (coating) was purchased from Sigma-Aldrich (Saint-Louis, MO, USA). Final % dimethyl sulfoxide (DMSO) in each well was 0.1%. Fresh concentrated stock solutions were prepared in DMSO immediately before first use and then kept at $-20\,°C$ for potential retesting. Stock solutions of 1000 fold the highest concentration were prepared (e.g. $1000 \times 10\,\mu M$ for Famotidine = 10 mM in DMSO) and were used to make the other stock solutions in 100% DMSO. These solutions were diluted 50 times in medium (10 µL stock in 490 µL of medium: 2% DMSO after dilution). Finally, 10 µL of these intermediate solutions were mixed with 190 µL of medium directly in each well (dilution 1/20) to reach a final 0.1% DMSO solution. Compounds were added only once. The mouse cardiomyocytes were exposed to eight concentrations of the cardiotoxic drugs (0.01, 0.03, 0.1, 0.3, 1, 3, 10, 100 µM) and four concentrations of Famotidine (0.1, 1, 10, 100 µM) for 24h. The cell index values presented in this manuscript were calculated from triplicate values (technical replicates) except for the cells exposed to DMSO (n = 6). For all experiments, the background reading was performed in presence of medium. The cells were monitored in real-time, at $37\,°C$ in a humidified 5% CO2/95% air atmosphere, using the multi-plate (96-well plate format) xCELLigence platform (Roche Diagnostics, Vilvoorde, Belgium). Cell index measurements occurred every 30 min until compound addition (usually from t=0 up to t = 2 to 3 days), every minute after compounds addition for the first 30 min and every 15 min for the last 23.5h. 20 s sweeps were used to collect cell index data at all steps described previously. Data analysis was performed using the algorithms developed by Cybernano and presented in this manuscript.

3. Cardio-Effect Estimation Method

An overview of the cardio-effect estimation method proposed in this article is presented in Figure 2. This approach is composed of four main steps developed in the next sections. The main output results generated by each computational step are indicated on the right part of the figure.

3.1. Morphological characterization of the CI response alteration

A behavioral characterization of the sweep signals is addressed in this section to detect and estimate the main changes in the CI responses caused by the

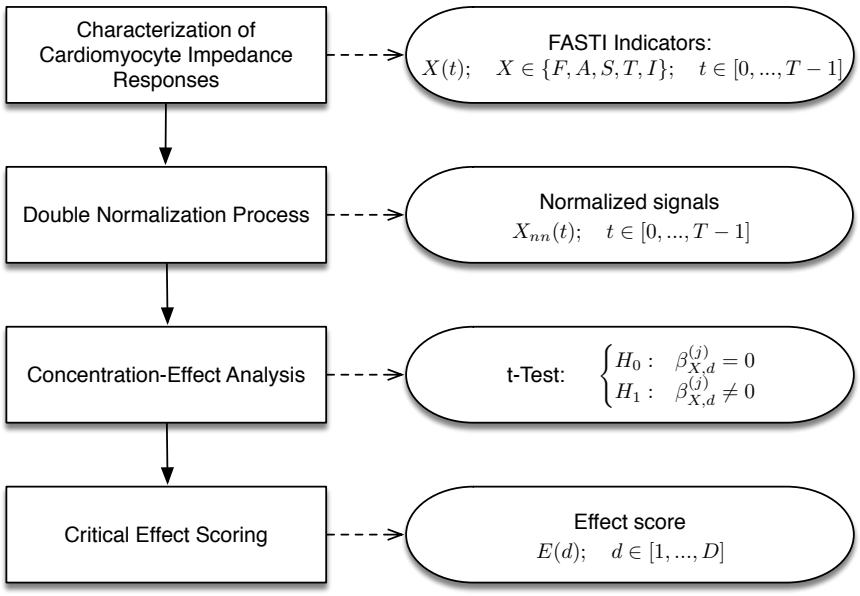

Figure 2: Overview of the method used to analyze the CI data. The proposed method is composed of four main steps and provides three major results. The FASTI indices answer two questions: when do the CI responses change and which parameters are altered? The concentration-effect analysis informs about which compound concentration significantly affect the contractibility parameters and viability trend. Finally, a global score is computed to compare the effects of each tested compound on the cardiomyocyte contractility.

tested molecules. The beating shape depends on cell environment and many biological factors such as the cell line, cell viability, medium type, compound and its concentration. As a consequence many different beating patterns can be observed as already emphasized by Jonsson *et al.* in [13] and Xi *et al.* in [12]. In this context, no model-based approach has been used due to the difficulty to find out a relevant and general model structure able to accurately fit all the possible shapes. An alternative solution consists in estimating parameters of the beating shape directly from the measured signals. In order to integrate all time dependent information, we propose to estimate for each sweep five time-indices, denoted FASTI thereafter :

- Frequency (F): estimate of the mean beating rate per minute in each sweep;
- Amplitude (A): average peak-to-trough magnitude in each sweep;
- Shape (S): score characterizing the shape of the mean beating pattern in each sweep;
- Trend (T): value obtained from the cell index trend signal informing about the cardiomyocyte viability status, spreading, ...

- Irregularity (I): score indicating how much the beat pattern is changing within each sweep.

Those five characteristics are calculated over the time range: $t \in [0, ..., T-1]$. For instance, Figures 3, 4 and 5 show the time evolution of the FASTI indices for the cardiomyocytes exposed to solvent (control condition) and to two molecules: Famotidine (negative control compound) and Sunitinib (positive control compound) respectively. The FASTI responses are correlated in the three examined cases but this correlation is not systematic and not been observed on other compounds. Moreover, some technical outliers such as peaks may intensify this effect.

3.1.1. Frequency

The Frequency characteristics informs about the evolution of the beating rate (bpm) over the experimentation period $[0; T-1]$, where T is the number of cardio sweeps. One usual technique used to estimate $F(t)$ is based on the detection of peaks. However, this approach is very sensitive to the noise and to avoid this drawback we propose to compute the maximum peak from the power spectral density (DSP). The latter is estimated by the Welch estimator based on the periodogram with windowing and averaging in order to reduce the variance of the estimates:

$$F(t) = \arg\max S_W(f, y_t) \tag{2}$$

$$S_W(f, y_t) = \frac{1}{P} \sum_{p=0}^{P-1} \frac{1}{||w||^2} \left| \sum_{m=0}^{M-1} w(m) y_t(pS + m) e^{-j2\pi fm} \right|^2, \tag{3}$$

where $w \in \mathbb{R}^M$ is a hamming window, M is the size of the window, and S/M represents the window overlapping. We choose $M = 192$ to get enough information in each window, and $S = 96$ to have 50% of overlaying. $p \in [0, ..., P]$ with P the total number of windows so that $pS + M \leq K$, with $P = 14$.

3.1.2. Amplitude

As the frequency, the peak-to-trough amplitude of the beating signal is a complementary parameter characterizing the cardiac activity. This feature is determined by subtracting the minimum value of the sweep to the maximum one:

$$A(t) = \max(y_t(k)) - \min(y_t(k)). \tag{4}$$

In practice, each sweep usually contains more than 20 beating waves. To avoid outliers on the estimation of the response peaks, we build a histogram of the cell index values and estimate $\min(y_t(k))$ and $\max(y_t(k))$ as the 3-rd and 97-th percentiles.

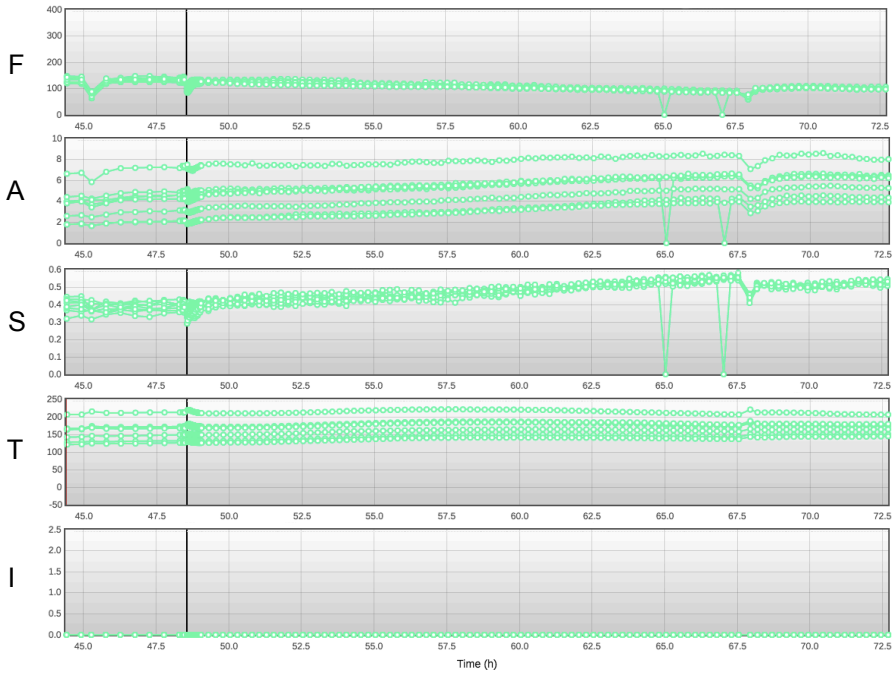

Figure 3: Overview of FASTI indices over time from cardiomyocytes exposed to solvent (control condition, 0.1% DMSO). Except for some rare events due to technical artefacts, the FASTI indices are stable, no significant change and no irregularity are detected in the 24h timeframe. The black vertical line indicates the time of the DMSO addition. Data are presented for six wells.

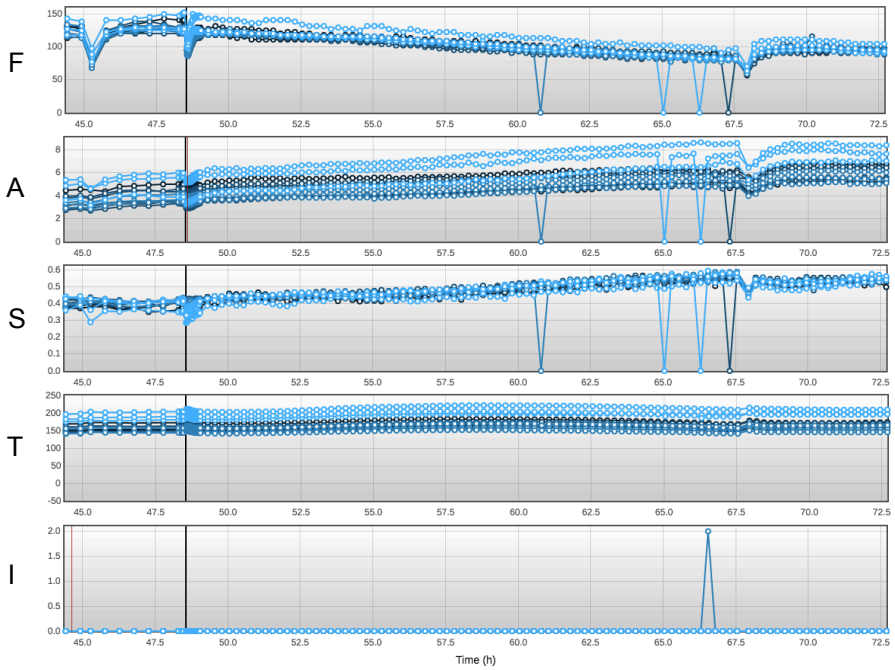

Figure 4: Overview of FASTI indices over time from cardiomyocytes exposed to Famotidine (non-cardiotoxic compound). Cardiomyocytes were exposed to three concentrations of Famotidine: $100nM$ (light blue), $1\mu M$ (medium blue), $10\mu M$ (dark blue) for 24h. Compound addition occurred at $t_m \approx 49h$ as indicated by the black vertical line. The different grade of blue are not always easy to observe due to the curve overlapping. Nine wells (triplicate condition for each concentration) of culture are examined. Except for some rare events due to technical artefacts, the FASTI indices are stable, no significant change and no irregularity are detected in the 24h timeframe.

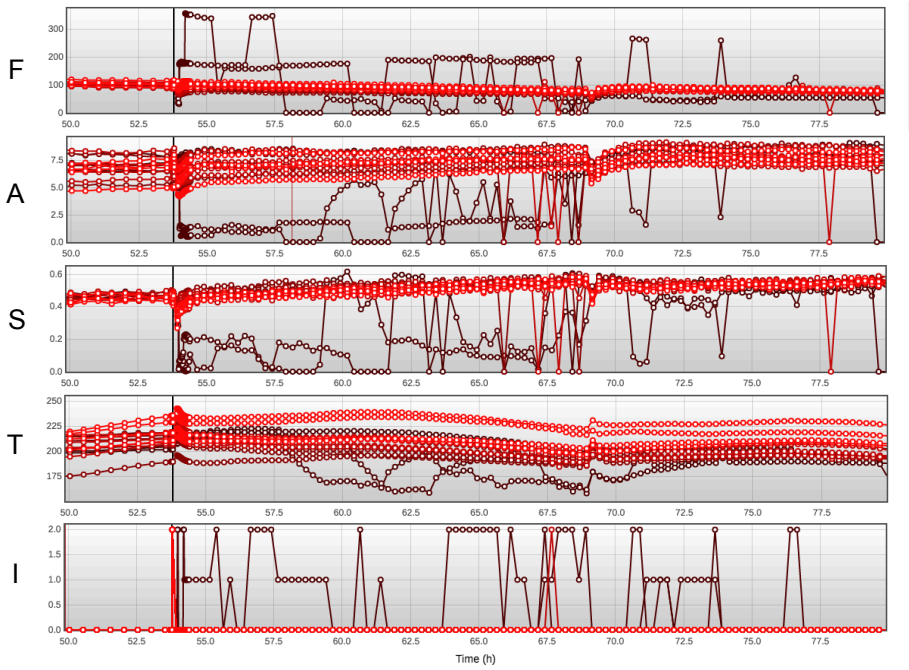

Figure 5: Overview of FASTI indices over time from cardiomyocytes exposed to Sunitinib (cardiotoxic compound). Cardiomyocytes were exposed to three concentrations of Sunitinib (positive control compound): $100nM$ (light red), $1\mu M$ (medium red), $10\mu M$ (dark red) for 24h. Compound addition occurred at $t_m \approx 53.5h$ as indicated by the black vertical line. Nine wells (triplicate condition for each concentration) of culture are examined. We clearly observe instability of amplitude, frequency and shape, acceleration of irregularities, and a drop of cardiomyocyte viability a few hours after Sunitinib administration.

3.1.3. Shape

When the characteristics $F(t), A(t)$ and $T(t)$ of two distinct wells are identical, their beating pattern can still be different in term of shape. While ECG are complex signals due to the heart structure, the cell index signal of cardiomyocyte monolayer cultures are usually simpler with generally one main peak. Our proposal is to capture the sharpness of the signal computed as:

$$S(t) = 1 - \frac{2}{A(t)} \min\big\{T(t) - \min(y_t(k)), \max(y_t(k)) - T(t)\big\}. \tag{5}$$

When $y_t(k)$ is periodic and symmetric (w.r.t its mean value) such as a sinusoidal signal, $S(t)$ tends to 0. On the contrary, in the absence of peaks (flat signal), $S(t)$ converges to 1. Otherwise, when $y_t(k)$ is not a symmetric beating pattern its value is between 0 and 1. The more symmetric the signal, the more S(t) is closed to 0. As with the A index, a robust estimation procedure is implemented to avoid any outlier on the computation of $\min(y_t(k))$ and $\max(y_t(k))$.

3.1.4. Trend

The viability of cardiomyocytes is derived from the CI data. At time t, the trend (T) is estimated by the empirical mean value of cell index over the t-th sweep :

$$T(t) = \frac{1}{K} \sum_{k=0}^{K-1} y_t(k). \tag{6}$$

3.1.5. Irregularity

The *Irregularity* time-characteristics $I(t)$ for the t^{th} recorded sweep is a discrete variable taking three possible values: $\{0, 1, 2\}$. If the beating pattern is regular all along the sweep $I(t) = 0$ but if it is drastically varying during the sweep time range then $I(t) = 2$. The intermediate value $I(t) = 1$ is associated with a moderate change of the beating shape. The computation of $I(t)$ relies on the mean energy of the measured signal:

$$E(k) = \sum_{n=k}^{k+P-1} |y_t(n)|^2, \tag{7}$$

where $k \in [0, ..., K - P - 1]$ and P is the number of time points in a beating period. Therefore, by considering a sliding window calculation, $E(k)$ becomes a new signal providing information about the variation of the mean energy within the sweep range. For a noise-free periodic signal, $E(k)$ is constant but in practice the CI values are noisy and $E(k)$ can be described as follows:

$$E(k) = a + e, \qquad e \sim \mathcal{N}(0, \sigma_e), \tag{8}$$

where the parameter a denotes the mean energy of the current sweep. From the likelihood function and the Fisher information of this model, we are able

to estimate a and σ_e and their corresponding standard errors. Given those estimates, the Table 2 describes the algorithm to compute $I(t)$. If one of the two variation coefficients cv_a and cv_{σ_e} are too large it implies that $E(k)$ is likely not a constant, *i.e.* y_t is irregular. A second irregularity index used to compute $I(t)$ is related to the noise-signal ratio R. Three example of irregularity values are presented in Figure 6. They show the ability of this index to detect different levels of beating irregularity within a cardio sweep.

No.	Step
1	compute $R = \hat{\sigma}_e/\hat{a}$
2	compute $cv_a = \hat{\sigma}_a/\hat{a}$
3	compute $cv_{\sigma_e} = \hat{\sigma}_{\sigma_e}/\hat{\sigma}_e$
4	if $(cv_a > 0.05)$ or $(cv_{\sigma_e} > 0.05)$ or $(R > s_2)$
	$I(t) = 2$
5	else if $s_2 \leq R < s_1$
	$I(t) = 1$
6	else
	$I(t) = 0$
	end if

Table 2: Algorithm used for the computation of the irregularity characteristic associated with the t^{th} sweep. s_1 ands_2 are two thresholds chosen by the user.

3.2. Normalization

For clarity, $X(t)$ is used thereafter to refer to one the four indices: $F(t)$, $A(t)$, $S(t)$, $T(t)$ because they received the same processing. Nevertheless, $I(t)$ is treated separately. To reduce the potential effects of uncontrolled variations between the wells and the plates, a double-step normalization process is applied to the previous time-indices.

3.2.1. Time normalization

The first normalization consists in fixing to zero all the indices at time t_m, *i.e.*: the time instant just before drug administration.

$$X_n(t) = X(t) - X(t_m - 1), \tag{9}$$

with $t \in [t_m, \cdots, t_m + \Delta t]$. t_m is selected based on the stability of the parameters usually obtained two days after cardiomyocyte seeding (time usually required to have a stabilization of the parameters). The study time frame was fixed to $\Delta t = 24h$.

3.2.2. Normalization

Since the goal of the study is to compare the drug effect with a control agent (vehicle compound), indices are centered and reduced as follows:

$$X_{nn}(t) = \frac{X_n(t) - \mu_c(t)}{\sigma_c(t)} \tag{10}$$

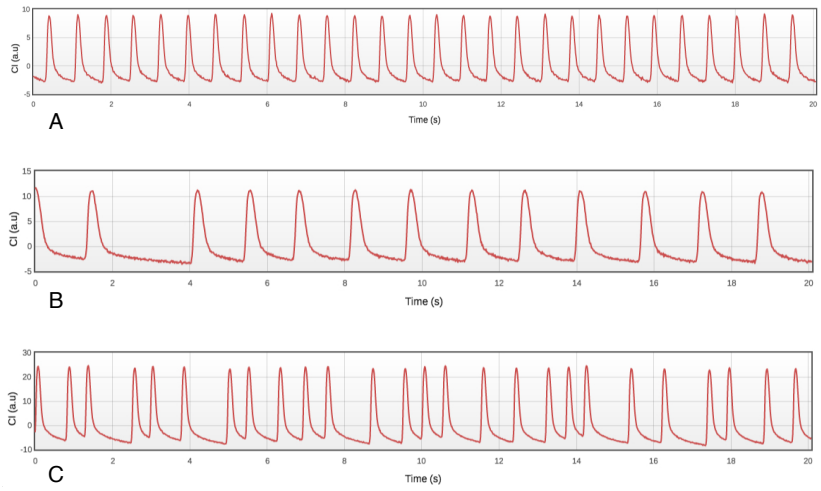

Figure 6: Examples of cardiomyocytes beating exposed to $33nM$ of Sunitinib (cardiotoxic drug). The beating profiles were obtained at three different time instants after its administration. They illustrate three distinct values of irregularity. A: $I = 0$ at $t = 65.79h$ (constant beating rate during the whole sweep); B: $I = 1$ at $t = 72.93h$ (prolongation of the beating period at the beginning of the sweep but the other peak-to-peak periods are constant); C: $I = 2$ at $t = 124.41h$ (the beating rate is inconstant during the sweep.

where $\mu_c(t)$ and $\sigma_c(t)$ are the empirical mean and standard-deviation of the control group.

3.3. Concentration-effect Analysis

To analyze how the normalized FASTI indices are changing with respect to the compound concentrations, a summary of the information contained in those meta-signals was performed. To that aim, we calculate two statistical summaries of X_{nn}, noted $S_{X,1}$ and $S_{X,2}$. $S_{X,1}$ is the root mean square value of X_{nn}:

$$S_{X,1} = \sqrt{\frac{1}{T}\sum_{t=0}^{T-1} X_{nn}(t)^2}. \tag{11}$$

When $S_{X,1}$ is near zero, X_{nn} is close to the reference profile (control). The second component, $S_{X,2}$, corresponds to the empirical standard deviation of the innovation term:

$$S_{X,2} = \sqrt{\frac{1}{T-1}\sum_{t=0}^{T-2} (X_{nn}(t+1) - X_{nn}(t))^2}. \tag{12}$$

In other terms, $S_{X,2}$ estimates the mean magnitude of the abrupt and chaotic variations of X_{nn}. When $S_{X,2}$ is close to zero, the profile of $X_{nn}(t)$ is regular and its value is increasing when $X_{nn}(t)$ becomes instable. For the irregularity characteristics $I(t)$, we use the proportion of irregularity of type 1 for $S_{I,1}$ and the total proportion of irregularity, that is type 1 and type 2, for $S_{I,2}$.

At this step, for each well, we have a total 10 statistics, *i.e.* 2 statistics for 5 indices. Now, we can group them by concentration for each tested compound. Each condition relative to the compounds is repeated in three different wells of the same plate. In such a context, statistical tests can be applied for each concentration level to decide whether significant differences exist between the tested compounds and the control group. An ANOVA test is used and the latter relies on the following model:

$$S_{X,j}(d,r) = \beta_{X,0}^{(j)} + \beta_{X,d}^{(j)} + \eta_{d,r}, \qquad \eta_{d,r} \sim \mathcal{N}(0,s) \tag{13}$$

where $X \in \{F, A, S, T\}$ refers to the FAST index, $j \in \{1, 2\}$ is the component index, $r \in \{1, \cdots, R\}$ is the replication index of the assays and $d \in \{1, \cdots, D\}$ is the d-th concentration level of the tested drug. $\eta_{d,r}$ refers to the unexplained intra-group variability. $\beta_{X,0}^{(j)}$ is the mean response of $S_{X,j}(0,r)$ for the null concentration ($d = 0$) and $\beta_{X,d}^{(j)}$ is the mean additive effect of the dose d on $S_{X,j}$. Once the parameters estimated, a T-test is performed and its p-value is used to decide whether or not the effect $\beta_{X,d}^{(j)}$ of the concentration level d is significantly different from 0. In this application, the significance threshold is fixed to $p = 0.01$. For the I index, a χ^2-test is applied to assess the effect of each concentration level in comparison with the null-concentration (vehicle) sample.

3.4. Effect scoring and modeling

Based on the results of the previous statistical tests, a score of critical effect $E(d)$ is calculated for each concentration d of the tested compound on the cell impedance responses. $E(d)$ is defined as follows:

$$E(d) = \sum_{j=1}^{2} \sum_{X \in \mathbb{I}} \mathbb{1}_{[p_{X,j,d} < 0.01]} \tag{14}$$

where $\mathbb{I} = \{F, A, S, T, I\}$, $\mathbb{1}$ is the index function and $p_{X,j,d}$ is the p-value associated with the statistical test of significance for the statistics $S_{X,j}$. E ranges from 0 (no effect) to 10 (strong effect). If the concentration effect is significant, a median-effect concentration (EC_{50}) is estimated by fitting a Hill model to the values of $E(d)$ [24]. This median-effect concentration will be used to compare the effects of compounds on the cardiomyocyte contractility. Nevertheless, when the score variation is abrupt, *e.g.* from 0 to 10 between two successive tested concentrations, the EC_{50} estimation based on the Hill model may be too uncertain. In that case, the experimenter is advised to test new concentrations within the appropriate variation range.

4. Effect of Test Compounds on Cardiomyocytes

In this section we present experimental results of the proposed statistical signal processing method applied to *in vitro* data obtained from cell impedance analysis. The objective was to assess the suitability of the proposed methodology to correctly discriminate the effects of Famotidine (non-cardiotoxic drug), Sunitinib and Doxorubicine (cardiotoxic drug in humans).

The global effect scores ($E(d)$), Hill model response (EC_{50} estimation) and the ten FASTI summary statistics ($S_{X,1}$ and $S_{X,2}$ in section 3.3) are presented in Figures 7,8 and 9 for the three tested compounds, respectively. Maximum therapeutic plasma concentrations of Sunitinib and Doxorubicin were obtained from Pharmapendium[3].

For Famotidine, we clearly observe no significant effect on the cardiomyocytes up to 100 µM equivalent to ca. 50 fold the maximum concentration in human blood (C_{max}). In humans, Famotidine (0.5 mg kg^{-1}) has a C_{max} value of 0.64 µg mL^{-1} (*i.e.* 1.90 µM) [25]. The global effect score remains under 1 in the tested concentration range and no significant variation of any FASTI index was detected. Some red dots appear in low concentration (100 µM) of Famotidine for $S_{A,1}$ but those not significant results can be ignored as not reproduced at higher concentrations. Although some cases of QT prolongation have been reported in humans (not in animals) [26], Famotidine does not inhibit hERG nor increases cardiac action potential *in vitro* [27]. Moreover, it does not affect cardiac contractility or heart rate in animals or in humans [28]. Therefore, the low global effect score well reflects the overall safe cardiac properties of Famotidine.

In the second example, Sunitinib was classified as a cardiotoxic drug. Its global score and FASTI indices show a significant alteration of the beating activity with a median effect concentration estimated to be EC_{50}=1.3 µM. The main cardiac effect of sunitinib is hypertension and left ventricular dysfunction, which has been reported in up to 12% metastatic carcinoma patients treated with this drug [29]. Bradycardia or QT prolongation are more rarely observed. C_{max} of Sunitinib has been reported to be 0.253 µM in humans (Guo *et al.* [4]). The ratio between the EC_{50} and C_{max} is only ca. 5 fold (1.3/0.253).

The last example deals with doxorubicin, an anthracycline drug widely used to treat a variety of tumours. Doxorubicin is a structural cardiotoxicant causing QT prolongation without acute cardiac ion channel such as hERG liability [30, 31]. It was recently proposed that doxorubicin-induced QT prolongation could be due to the direct inhibition of IKs (a slowly activating component of delayed rectifier $K+$ channel) [30]. This examples illustrates the danger of neglecting I(Ks) in favor of hERG screening alone, for early preclinical testing for possible induction of torsade de pointes [30]. Doxorubicin has a maximum therapeutic plasma concentration of 15.34 µM [31, 32]. In the present study, a EC_{50} of 9.7 µM is reported in mouse cardiomyocytes, which is even below the clinical efficacious plasma concentration of doxorubicin. In other words, these

[3] https://www.pharmapendium.com

results suggest that doxorubicin has the potential to induce cardiotoxicity at the efficacious concentration in human.

5. Conclusion

In the context of the CiPA initiative, this paper addresses the identification problem of new biosignal markers able to predict the risk of molecules to potentially disturb the contractility of cardiomyocytes. The proposed and developed approach deals with a statistical signal processing method that provides to biologists three levels of information.

It firstly computes five indices informing about the time variations of irregularity, frequency, amplitude and shape of beatings but also an estimation of the cardiomyocyte viability. That first step allows to speed up the analysis of cardiomyocyte RTCA data. Indeed, instead of analyzing individual time points, the FASTI indices bring a global overview of the cardiomyocyte behavioral characteristics and allow to quickly identify subtle changes over time.

In a second step, two summary statistics of the FASTI indices are computed over all the experimental time range and are used to test dose response relationship. Those two additional attributes provide clarifications about the threshold concentration effects of each molecule. The Student's t-test is used to detect the statistical significance of each concentration effect with respect to a given control.

A global cardio-effect score is finally proposed to compare the alteration effects of the tested pharmaceutical agents on the cardiomyocyte contractility. To this aim, we have proposed a new cardio-effect scale graduated from 0 (no influence) to 10 (critical effect). This approach allows thus to compare different compounds on the same diagram.

To assess its practical relevance, the proposed approach was applied to the cardiomyocyte impedance data of three known compounds. Compared to recent results, these preliminary results have corroborated the ability of the proposed method to efficiently discriminate the effects of the tested drugs. The main advantage of this approach is to provide rapid and reliable analysis of complex signals. The complete approach was implemented on a web-platform: i-Cardio™[4] and is now available for all users of the RTCA technologies.

Finally, to confirm the validity of the proposed approach, the next step will evaluate this new method to a larger batch of molecules. In particular, we will address the potential correlations between the results provided by such data-driven modeling approaches and the underlying biological phenomena associated with cardiotoxicity.

[4] `https://www.cybernano.eu/i-cardio`

References

[1] I. Cavero, H. Holzgrefe, Comprehensive in vitro Proarrhythmia Assay, a novel in vitro/in silico paradigm to detect ventricular proarrhythmic liability: a visionary 21st century initiative, Expert Opinion on Drug Safety 13 (6) (2014) 745–758. doi:{10.1517/14740338.2014.915311}.

[2] B. Fermini, J. C. Hancox, N. Abi-Gerges, M. Bridgland-Taylor, K. W. Chaudhary, T. Colatsky, K. Correll, W. Crumb, B. Damiano, G. Erdemli, G. Gintant, J. Imredy, J. Koerner, J. Kramer, P. Levesque, Z. Li, A. Lindqvist, C. A. Obejero-Paz, D. Rampe, K. Sawada, D. G. Strauss, J. I. Vandenberg, A New Perspective in the Field of Cardiac Safety Testing through the Comprehensive In Vitro Proarrhythmia Assay Paradigm, Journal of Biomolecular Screening 21 (1) (2016) 1–11. doi:{10.1177/1087057115594589}.

[3] T. O'Hara, L. Virág, A. Varró, Y. Rudy, Simulation of the undiseased human cardiac ventricular action potential: Model formulation and experimental validation, PLOS Computational Biology 7 (5) (2011) 1–29. doi:10.1371/journal.pcbi.1002061.
URL http://dx.doi.org/10.1371%2Fjournal.pcbi.1002061

[4] Q. Guo, T. Chen, Y. Chen, L. Li, W. Hu, Microarchitectural design space exploration made fast, Microprocessors and Microsystems 37 (1) (2013) 41 – 51. doi:10.1016/j.micpro.2012.07.006.
URL http://www.sciencedirect.com/science/article/pii/S0141933112001433

[5] S. S. Mahmoud, Z. M. Hussain, I. Cosic, Q. Fang, Time-frequency analysis of normal and abnormal biological signals, Biomedical Signal Processing and Control 1 (1) (2006) 33–43. doi:{10.1016/j.bspc.2006.02.001}.

[6] R. J. Martis, U. R. Acharya, H. Adeli, H. Prasad, J. H. Tan, K. C. Chua, C. L. Too, S. W. J. Yeo, L. Tong, Computer aided diagnosis of atrial arrhythmia using dimensionality reduction methods on transform domain representation, Biomedical Signal Processing and Control 13 (2014) 295–305. doi:{10.1016/j.bspc.2014.04.001}.

[7] C. Lin, G. Kail, A. Girernus, C. Mailhes, J.-Y. Tourneret, F. Hlawatsch, Sequential beat-to-beat P and T wave delineation and waveform estimation in ECG signals: Block Gibbs sampler and marginalized particle filter, Signal Processing 104 (2014) 174–187. doi:{10.1016/j.sigpro.2014.03.011}.

[8] L. N. Sharma, R. K. Tripathy, S. Dandapat, Multiscale Energy and Eigenspace Approach to Detection and Localization of Myocardial Infarction, IEEE Transactions on Biomedical Engineering 62 (7) (2015) 1827–1837. doi:{10.1109/TBME.2015.2405134}.

[9] S. Farashi, A multiresolution time-dependent entropy method for QRS complex detection, Biomedical Signal Processing and Control 24 (2016) 63–71. doi:{10.1016/j.bspc.2015.09.008}.

[10] E. K. Roonizi, R. Sassi, A Signal Decomposition Model-Based Bayesian Framework for ECG Components Separation, IEEE Trans. Signal Processing 64 (3) (2016) 665–674. doi:{10.1109/TSP.2015.2489598}.

[11] M. Yochum, C. Renaud, S. Jacquir, Automatic detection of P, QRS and T patterns in 12 leads ECG signal based on CWT, Biomedical Signal Processing and Control 25 (2016) 46–52. doi:{10.1016/j.bspc.2015.10.011}.

[12] B. Xi, T. Wang, N. Li, W. Ouyang, W. Zhang, J. Wu, X. Xu, X. Wang, Y. A. Abassi, Functional Cardiotoxicity Profiling and Screening Using the xCELLigence RTCA Cardio System, JALA 16 (6, SI) (2011) 415–421. doi:{10.1016/j.jala.2011.09.002}.

[13] M. K. B. Jonsson, Q.-D. Wang, B. Becker, Impedance-Based Detection of Beating Rhythm and Proarrhythmic Effects of Compounds on Stem Cell-Derived Cardiomyocytes, Assay and Drug Development Technologies 9 (6) (2011) 589–599. doi:{10.1089/adt.2011.0396}.

[14] I. Giaever, C. R. Keese, Monitoring fibroblast behavior in tissue culture with an applied electric field, Proceedings of the National Academy of Sciences 81 (12) (1984) 3761–3764. arXiv:http://www.pnas.org/content/81/12/3761.full.pdf+html.
URL http://www.pnas.org/content/81/12/3761.abstract

[15] I. Giaever, C. R. Keese, Micromotion of mammalian cells measured electrically, Proceedings of the National Academy of Sciences 88 (17) (1991) 7896–7900. arXiv:http://www.pnas.org/content/88/17/7896.full.pdf+html.
URL http://www.pnas.org/content/88/17/7896.abstract

[16] Y. A. Abassi, B. Xi, W. Zhang, P. Ye, S. L. Kirstein, M. R. Gaylord, S. C. Feinstein, X. Wang, X. Xu, Kinetic cell-based morphological screening: Prediction of mechanism of compound action and off-target effects, Chemistry & Biology 16 (7) (2009) 712 – 723. doi:http://dx.doi.org/10.1016/j.chembiol.2009.05.011.
URL http://www.sciencedirect.com/science/article/pii/S1074552109001811

[17] F. A. Atienzar, H. Gerets, K. Tilmant, G. Toussaint, S. Dhalluin, Evaluation of impedance-based label-free technology as a tool for pharmacology and toxicology investigations, Biosensors 3 (1) (2013) 132–156.

[18] J. Wegener, C. R. Keese, I. Giaever, Electric cell-substrate impedance sensing (ecis) as a noninvasive means to monitor the kinetics of cell spreading to artificial surfaces, Experimental Cell Research 259 (1) (2000)

158 – 166. doi:10.1006/excr.2000.4919.
URL http://www.sciencedirect.com/science/article/pii/S001448270094919X

[19] C. Xiao, B. Lachance, G. Sunahara, J. H. T. Luong, Assessment of cytotoxicity using electric cell-substrate impedance sensing: Concentration and time response function approach, Analytical Chemistry 74 (22) (2002) 5748–5753, pMID: 12463358. arXiv:http://pubs.acs.org/doi/pdf/10.1021/ac025848f, doi:10.1021/ac025848f.
URL http://pubs.acs.org/doi/abs/10.1021/ac025848f

[20] F. A. Atienzar, K. Tilmant, H. H. Gerets, G. Toussaint, S. Speeckaert, E. Hanon, O. Depelchin, S. Dhaluin, The Use of Real-Time Cell Analyzer Technology in Drug Discovery: Defining Optimal Cell Culture Conditions and Assay Reproducibility with Different Adherent Cellular Models, Journal of Biomolecular Screening 16 (6) (2011) 575–587. doi:{10.1177/1087057111402825}.

[21] Y. A. Abassi, J. A. Jackson, J. Zhu, J. OConnell, X. Wang, X. Xu, Label-free, real-time monitoring of ige-mediated mast cell activation on microelectronic cell sensor arrays, Journal of Immunological Methods 292 (2004) 195 – 205. doi:http://dx.doi.org/10.1016/j.jim.2004.06.022.
URL http://www.sciencedirect.com/science/article/pii/S0022175904002364

[22] J. M. Atienza, J. Zhu, X. Wang, X. Xu, Y. Abassi, Dynamic monitoring of cell adhesion and spreading on microelectronic sensor arrays, Journal of Biomolecular Screening 10 (8) (2005) 795–805. arXiv:http://jbx.sagepub.com/content/10/8/795.full.pdf+html, doi:10.1177/1087057105279635.
URL http://jbx.sagepub.com/content/10/8/795.abstract

[23] J. Z. Xing, L. Zhu, J. A. Jackson, S. Gabos, X.-J. Sun, X.-b. Wang, X. Xu, Dynamic monitoring of cytotoxicity on microelectronic sensors, Chemical Research in Toxicology 18 (2) (2005) 154–161. arXiv:http://pubs.acs.org/doi/pdf/10.1021/tx049721s, doi:10.1021/tx049721s.
URL http://pubs.acs.org/doi/abs/10.1021/tx049721s

[24] J. L. Sebaugh, Guidelines for accurate ec50/ic50 estimation, Pharmaceutical Statistics 10 (2) (2011) 128–134. doi:10.1002/pst.426.
URL http://dx.doi.org/10.1002/pst.426

[25] L. James, T. Marotti, C. Stowe, H. Farrar, B. Taylor, G. Kearns, Pharmacokinetics and pharmacodynamics of famotidine in infants. (vol 38, pg 1089, 1998), Journal of Clinical Pharmacology 40 (11) (2000) 1298.

[26] H. M. Vargas, A. S. Bass, J. Koerner, S. Matis-Mitchell, M. K. Pugsley, M. Skinner, M. Burnham, M. Bridgland-Taylor, S. Pettit, J.-P. Valentin, Evaluation of drug-induced QT interval prolongation in animal and human

studies: a literature review of concordance, British Journal of Pharmacology 172 (16) (2015) 4002–4011. doi:{10.1111/bph.13207}.

[27] Y. Nakamura, A. Takahara, A. Sugiyama, Famotidine neither affects action potential parameters nor inhibits human ether-a-go-go-related gene (hERG) K+ current, Journal of Toxicological Sciences 34 (5) (2009) 563–567.

[28] E. Melzer, E. Bardan, Z. Krepel, S. Bar-Meir, Famotidine has no effect on cardiac performance and liver blood flow in the rat, Research in experimental medicine 194 (1) (1994) 179–184.

[29] C. Kollmannsberger, D. Soulieres, R. Wong, A. Scalera, R. Gaspo, G. Bjarnason, Sunitinib therapy for metastatic renal cell carcinoma: recommendations for management of side effects, Canadian Urological Association Journal 1 (2) (2007) 41–54.

[30] J. Ducroq, H. Moha ou Maati, S. Guilbot, S. Dilly, E. Laemmel, C. Pons-Himbert, J. Faivre, P. Bois, O. Stücker, M. Le Grand, Dexrazoxane protects the heart from acute doxorubicin-induced qt prolongation: a key role for iks, British journal of pharmacology 159 (1) (2010) 93–101.

[31] L. Guo, L. Coyle, R. M. C. Abrams, R. Kemper, E. T. Chiao, K. L. Kolaja, Refining the human ipsc-cardiomyocyte arrhythmic risk assessment model, Toxicological Sciences 136 (2) (2013) 581. arXiv:/oup/backfile/Content_public/Journal/toxsci/136/2/10.1093/toxsci/kft205/2/kft205.pdf, doi:10.1093/toxsci/kft205. URL +http://dx.doi.org/10.1093/toxsci/kft205

[32] A. Pointon, N. Abi-Gerges, M. J. Cross, J. E. Sidaway, Phenotypic profiling of structural cardiotoxins in vitro reveals dependency on multiple mechanisms of toxicity, toxicological sciences 132 (2) (2013) 317–326.

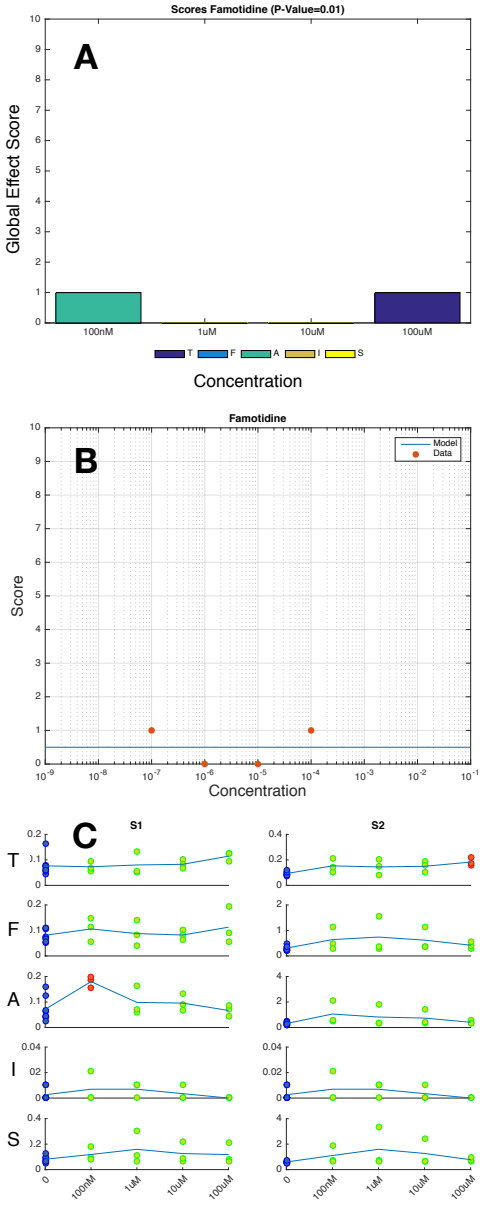

Figure 7: Summary of concentration-effects induced by Famotidine on mouse cardiomyocytes. A. Global effect scores. Minimum score (0) means that the FASTI parameters are not significantly different compared to control data (cardiomyocytes exposed to 0.1% DMSO). A score of 10 corresponds to severe effects often manifested by a beating arrest of the cardiomyocytes. Highest score for Famotidine is 1. B. Estimated EC_{50} value (no data reported up to 100 µM). C. FASTI indices: blue dots correspond to control values, green dots indicate no significant change w.r.t. control and red dots point out significant changes compared to control data. Each time red dots are detected, the global effect score is increased by one unit.

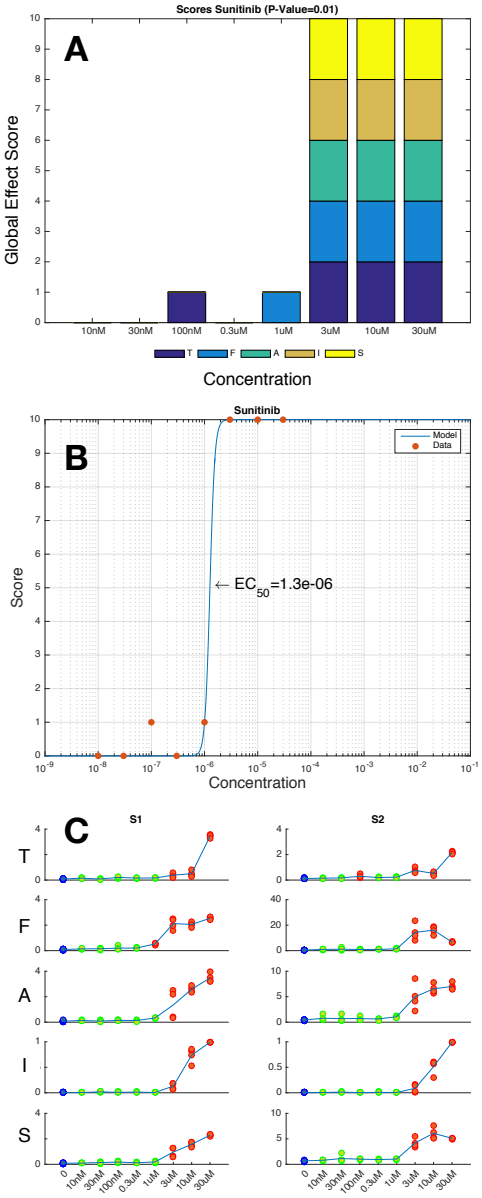

Figure 8: Summary of concentration-effects induced by Sunitinib on mouse cardiomyocytes. A. Global effect scores. Minimum score (0) means that the FASTI parameters are not significantly different compared to control data (cardiomyocytes exposed to 0.1% DMSO). A score of 10 corresponds to severe effects often manifested by a beating arrest of the cardiomyocytes. Highest score for Sunitinib is 10. B. EC_{50} value is estimated between 1 µM and 3 µM. Since the variation of the global score is abrupt, the EC_{50} estimated value provided by the Hill model (1.3 µM) is uncertain. C. FASTI indices: blue dots correspond to control values, green dots indicate no significant change w.r.t. control and red dots point out significant changes compared to control data. Each time red dots are detected, the global effect score is increased by one unit.

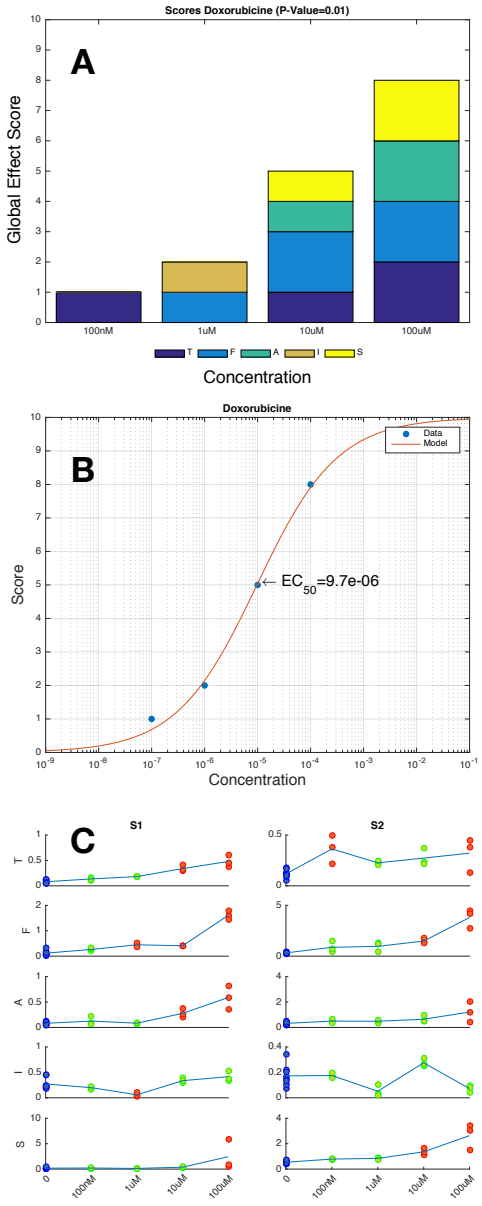

Figure 9: Summary of concentration-effects induced by Doxorubicine on mouse cardiomyocytes. A. Global effect scores. Minimum score (0) means that the FASTI parameters are not significantly different compared to control data (cardiomyocytes exposed to 0.1% DMSO). A score of 10 corresponds to severe effects often manifested by a beating arrest of the cardiomyocytes. Highest score for Doxorubicine is 8. B. Estimated EC_{50} values: 9.7 µM for Doxorubicine. C. FASTI indices: blue dots correspond to control values, green dots indicate no significant change w.r.t. control and red dots point out significant changes compared to control data. Each time red dots are detected, the global effect score is increased by one unit.